

Development of Organic–Inorganic Nanostructure Labels for Food-poisoning Bacteria

Shogo Nakamura,¹ Akihiro Nakao,¹ Satohiro Itagaki,¹ Kyohei Matsui,¹
Shigeki Nishii,¹ Xueling Shan,² Yojiro Yamamoto,¹
Yasuhiro Sadanaga,¹ Zhidong Chen,² and Hiroshi Shiigi^{1*}

¹Department of Applied Chemistry, Osaka Metropolitan University,
Sakai 599-8570, Japan

²Jiangsu Key Laboratory of Advanced Catalytic Materials and Technology, Changzhou University,
Changzhou 213164, China

(Received April 17, 2023; accepted September 22, 2023)

Keywords: *Staphylococcus aureus*, copper nanostructures, electrochemical labels, organic–inorganic hybrids, food-poisoning bacteria

In this paper, we describe a simple strategy to detect food-poisoning bacteria using the spectroscopic and electrochemical properties of organic–inorganic nanostructures composed of electrically conductive polyaniline-coated copper nanoparticles. Antibody-introduced nanostructures specifically bind to cells via antigens and function as nanometer-sized labels. Attempting the quantification of *Staphylococcus aureus* using nanostructure labels, we found that the absorbance of the free label in the supernatant decreased as the number of bacterial cells increased, indicating that the labeled cells were obtained as precipitates. Furthermore, the peak current (I_p) based on the number of labels bound to cells on the electrode increased with the number of bacterial cells. Thus, the introduction of antibodies into nanostructures has made it possible to electrochemically and spectroscopically quantify the causative bacteria of food poisoning.

1. Introduction

More than 200 diseases are known to be caused by the foodborne transmission of various pathogens, including bacteria, viruses, and parasites.⁽¹⁾ The prevention of diseases associated with foodborne pathogens remains a major public health challenge, but the risk of foodborne diseases, particularly those caused by *Salmonella*, *Escherichia coli*, and *Staphylococcus aureus*, has increased significantly.^(2–4) To reduce those risks, bacteriological examinations have become important. Most bacteriological tests are performed by colony counting with culture on agar plates. This method is time-consuming, requiring 2–3 days for initial results and up to a week or more for the confirmation of specific pathogenic organisms.^(5,6) In recent years, rapid tests using polymerase chain reaction (PCR), enzyme-linked immunosorbent (ELISA), and

*Corresponding author: e-mail: shii@omu.ac.jp

<https://doi.org/10.18494/SAM4432>

immunoassay have been extensively studied. The PCR method is the best-known and established nucleic acid amplification method.^(7,8) In this method, double-stranded DNA is denatured into single strands, specific primers are annealed to these DNA strands, and primers complementary to the single-stranded DNA are extended by a thermostable DNA polymerase. These steps are repeated, doubling the target sequence to the initial number in each cycle.^(9,10) ELISA is based on the antibody-sandwich technique, in which a food pathogen antigen specifically bound to a support-immobilized antibody is combined with an enzymatically conjugated secondary antibody. This method is useful because it is accurate, sensitive, and specific.^(11–14) However, these two methods have problems in that they are complicated to operate and difficult to introduce into the field owing to the need for large-scale and expensive equipment. On the other hand, in immunoassay, the lateral flow test strip immunoassay using gold nanoparticle labels is known as a simple and inexpensive method. As the sample fluid flows laterally across the test strip, the antibody-immobilized gold nanoparticles interact with target analytes within the fluid and subsequently aggregate at the test line owing to specific interactions between the antigen and the antibody. At this time, the test line is colored by the localized surface plasmons of the gold nanoparticles. This method is rapid and simple, but the quantification is difficult and the detection limit is high ($>10^5$ cells/mL).⁽¹⁵⁾ We previously reported that in a mixed solution of aniline and metal ions, the polymerization and nanoparticle formation reactions proceed simultaneously in the same reaction field, forming nanometer-sized organic–inorganic hybrid particles.^(16,17) Furthermore, we clarified that these organic–inorganic hybrid particles have optical and electrochemical characteristics.^(18–23) In this study, we utilized this method to form copper nanostructures. As the nanostructures exhibit characteristic electrochemical properties based on copper nanoparticles, we used them as electrochemical labels to detect *S. aureus*. The binding properties of the nanostructures to bacterial cells were evaluated spectroscopically and electrochemically.

2. Materials and Methods

2.1 Bacterial culture and sample preparation

S. aureus was purchased from the National Institute of Technology and Evaluation Biological Resource Center (NBRC, Japan). Bacterial cultures and experiments were performed in a biosafety level 2 laboratory and were developed and managed in accordance with the appropriate safety regulations (WHO Laboratory Biosafety Manual). The bacterial strain was cultured in an agar growth medium (E-MC35, Eiken Chemical Co., Japan) for 18 h. A single colony was then selected and placed in a liquid growth medium and incubated for 18 h. The suspension cultures were then centrifuged for 5 min, and the precipitate was resuspended in sterilized ultrapure water by shaking for 1 min.

2.2 Preparation of copper nanostructures

The ultrapure water (>18 M Ω) used in this experiment was sterilized using UV light. In addition, reagent-grade chemicals such as copper(II)sulfate pentahydrate, aniline, and ethanol

were used for the preparation of copper nanostructures, all of which were purchased from Fujifilm Wako Chemicals, Co. (Japan). An aqueous copper sulfate solution and a 0.10 M aniline ethanol solution were added to the ultrapure water, stirred at 298 K for 30 min, and then centrifuged. The supernatant was disposed to remove unreacted substances and the precipitate was dispersed in ultrapure water. The obtained dispersion was ultrafiltrated to obtain copper nanostructures. The size distribution of the nanostructures in ultrapure water was measured with a zeta-potential and particle size analyzer (ELSZ-2Plus, Otsuka Electronics, Japan).

2.3 Immobilization of antibodies on copper nanostructures

The goat anti-*S. aureus* antibody (Kirkegaard & Perry Laboratories, Inc., U.S.) was immobilized on copper nanostructures using *N*-hydroxy-succinimide sodium salt (NHS) and 1-ethyl-3-(3-dimethylaminopropyl) carbodiimide hydrochloride (EDC) as a cross-linking agent. EDC and NHS were added to an anti-*S. aureus* antibody and stirred for 30 min. Phosphate-buffered saline (PBS, pH 7.0) was added to the mixed solution and centrifuged to obtain the EDC/NHS-modified antibody. Copper nanostructure dispersion was added to the EDC/NHS-modified antibody and stirred for 2 h.

2.4 Optical characterization of copper nanostructures

Copper nanostructures were observed using a transmission electron microscope (TEM, JEM-2000FXII, JEOL, Japan) at an acceleration voltage of 200 kV. Bacterial cells labeled with copper nanostructures were observed using a field emission scanning electron microscope (FE-SEM, SU8010, Hitachi High-Tech, Japan) at an acceleration voltage of 5 kV.

2.5 Pretreatment of carbon chip electrodes

In this experiment, a carbon chip electrode was used as shown in Fig. 1. Carbon ink was used to screen-print the working, reference, and counter electrodes onto the resin substrate. The Ag/

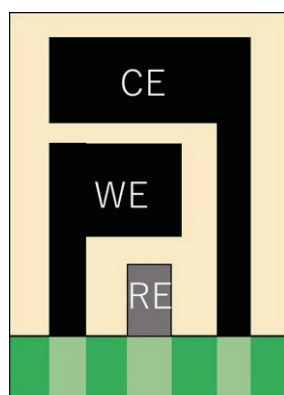


Fig. 1. (Color online) Illustration of carbon chip electrode.

AgCl ink was applied to the reference electrode and allowed to dry for 5 min. After that, the resist portion of the carbon chip electrode was masked with a Teflon tape, and plasma was irradiated at 10 mA for 1 min.

2.6 Electrochemical and absorbance measurements

The prepared *S. aureus* (10^6 – 10^9 cells mL⁻¹) and anti-*S. aureus* antibody-conjugated copper nanostructures were mixed and stirred for 15 min. Then, each mixed dispersion was centrifuged at 6,100 rpm ($3,500 \times g$) and 278 K for 30 min. The spectrum of the obtained supernatant was measured with an ultraviolet-visible spectrophotometer (V-750, JASCO, Japan). The obtained precipitate was dispersed in ultrapure water and then again centrifuged under the same conditions as above (hereinafter called “washing operation”). The obtained supernatant was also subjected to spectral measurement. The precipitate thus washed was dispersed in ultrapure water. Three microliters of the dispersion was dropped onto the working electrode on the carbon chip electrode and vacuum-dried at 298 K for 1 h. Fifty microliters of PBS was dropped on the carbon chip electrode, and cyclic voltammetry (CV) and differential pulse voltammetry (DPV) were carried out by potential scanning from -0.2 to $+0.2$ V using a potentiostat-galvanostat ECstat-302 (EC Frontier Inc., Japan) under the following conditions: initial potential, -0.2 V; initial scan direction, positive. CV was performed by repeating three cycles of potential scans.

3. Results and Discussion

Copper nanostructures were obtained as a bluish dispersion consisting of spheres with a mean diameter of 146.4 ± 41.3 nm. In the TEM image, a structure in which numerous small copper nanoparticles are tightly encapsulated inside the polymer was observed with distinctly different contrasts [Fig. 2(a)]. In the SEM image, it was confirmed that the copper nanostructures bound to the bacterial cells [Fig. 2(b)]. This indicates that the antibodies introduced into the nanostructure bound to the cell surface through specific binding with the antigen.

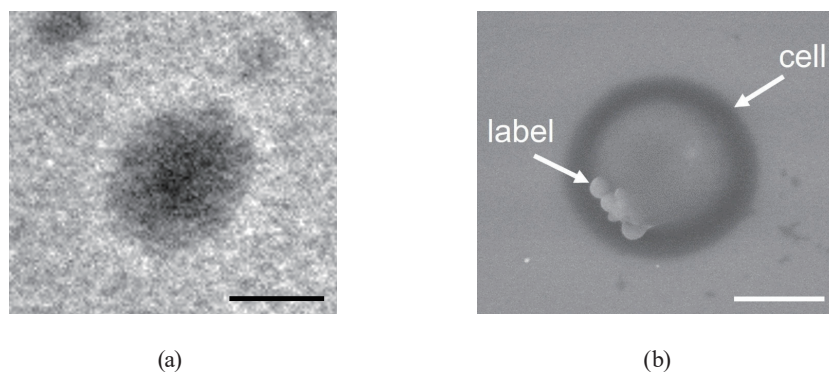


Fig. 2. (a) TEM image of copper nanostructure. The scale bar is 100 nm. (b) SEM image of copper-nanostructure-labeled cell. The scale bar is 500 nm.

In CV and DPV, current responses derived from two-step oxidation reactions of Cu^0 to Cu(I) and Cu(I) to Cu(II) were observed (Fig. 3).⁽²⁴⁾ This indicates that the nanostructures not only function as electrochemical labels but also hold the copper nanoparticles in a stable form. The decrease in current response with increasing number of cycles was attributed to the oxidation of Cu^0 in the nanostructures and Cu^{2+} diffused into the electrolyte [Fig. 3(a)]. The current response at +0.08 V based on the oxidation reactions of Cu(I) into Cu(II) was observed prominently in DPV [Fig. 3(b)].

The presence of polyaniline with a low degree of polymerization made it possible to introduce antibodies into the nanostructures via an amide coupling reaction.^(16,21) It was easily predicted that antibody-introduced nanostructures would specifically bind to cells via the antigen and function as labels. Specific binding proceeded spontaneously in the mixture of labels and target bacterial cells. Centrifuging the mixture of *S. aureus* (1.0×10^9 cells mL^{-1}) and labels yielded a bluish supernatant [Fig. 4(A-a)]. This indicated that there were free labels that were unbound to the cells. On the other hand, the supernatant after the washing operation became colorless and transparent [Fig. 4(A-b)]. At this time, the resulting bluish precipitate originating from the copper nanostructures was obtained, confirming the binding of the label to the target bacterial cells. To investigate the nonspecific adsorption of nanostructures to bacterial cells, absorbance and electrochemical measurements were performed using copper nanostructures without antibody modification. A slight absorption peak at 620 nm derived from the copper nanostructure was observed in the supernatant after the washing operation. This is due to the exfoliation of copper nanostructures nonspecifically adsorbed to bacterial cells. Nonspecifically adsorbed copper nanostructures were removed by washing, but it was presumed that some of them were still adsorbed. However, the precipitates did not exhibit the current response attributed to the copper nanostructures. It was suggested that nonspecific adsorption was completely inhibited or did not affect electrochemical measurements owing to sensitivity.

A significant absorption peak was observed at 620 nm in the absorption spectrum of the mixed dispersion of bacterial cells and labels. The peak intensity did not change even when the number of bacterial cells was increased. Therefore, centrifugation was performed to separate

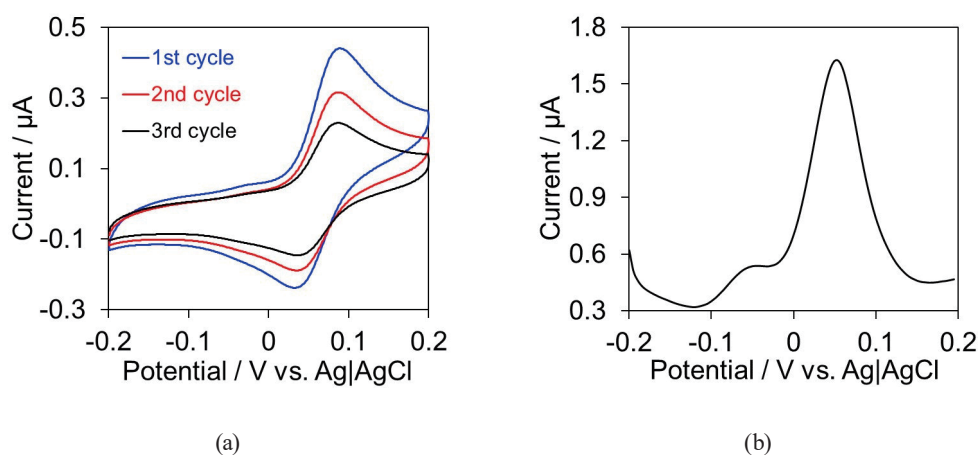


Fig. 3. (Color online) (a) CV and (b) DPV results of copper nanostructures in PBS (pH 7.0).

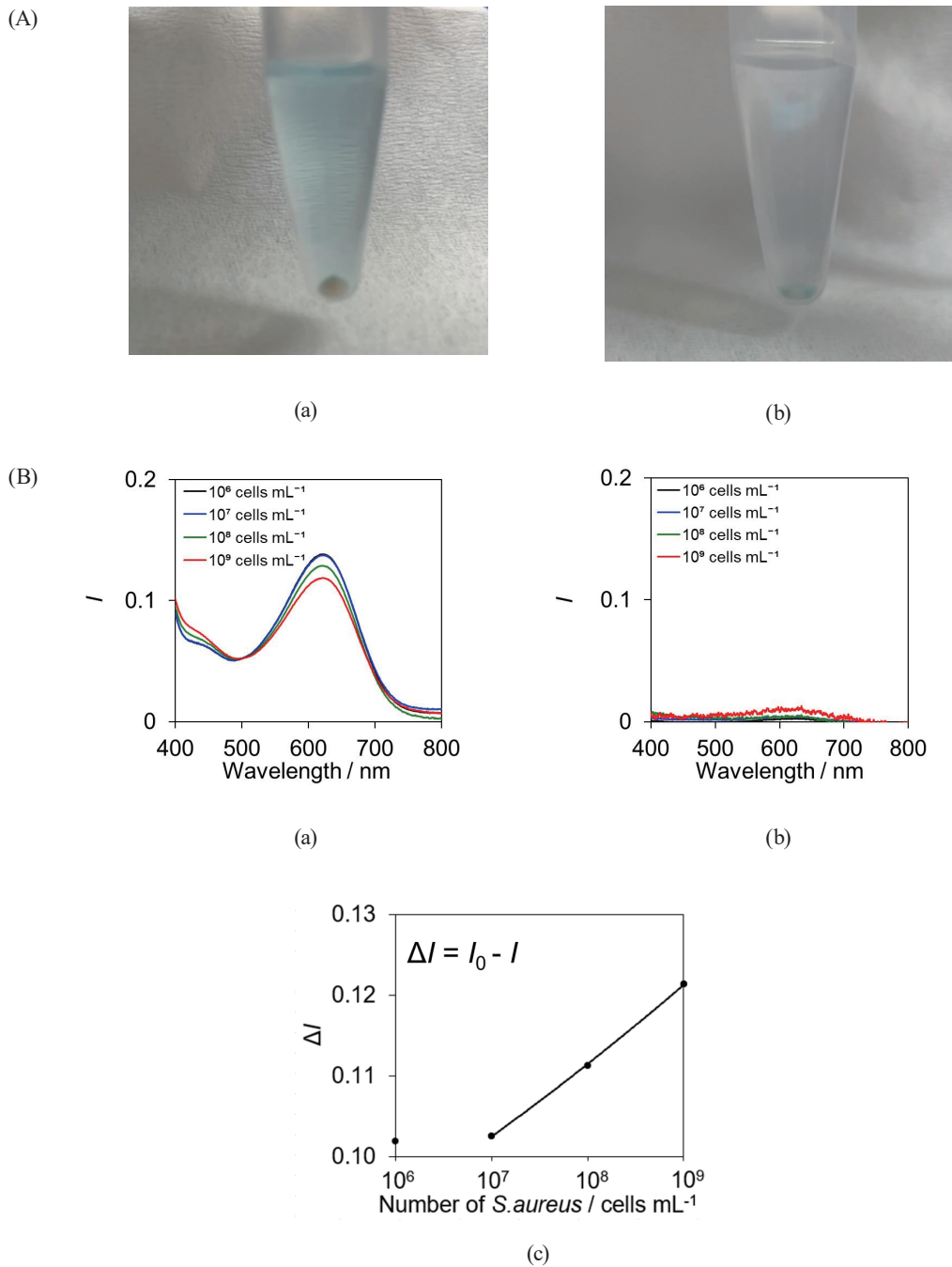


Fig. 4. (Color online) (A) Photos and (B) absorbance spectra of the mixture of bacterial cells and labels (a) before and (b) after the washing operation, and (c) plot of ΔI at 620 nm before the washing operation. ΔI was obtained by subtracting the peak intensity of the supernatant at the number of each bacteria (I) from that without bacteria ($I_0 = 0.24$).

unbound free labels and nonspecifically adsorbed labels from labeled bacterial cells. A prominent absorption peak was also obtained at 620 nm in the absorption spectrum in the supernatant, and the peak intensity decreased as the number of bacterial cells increased [Fig. 4(B-a)]. On the other hand, in the absorption spectrum of the supernatant after the washing

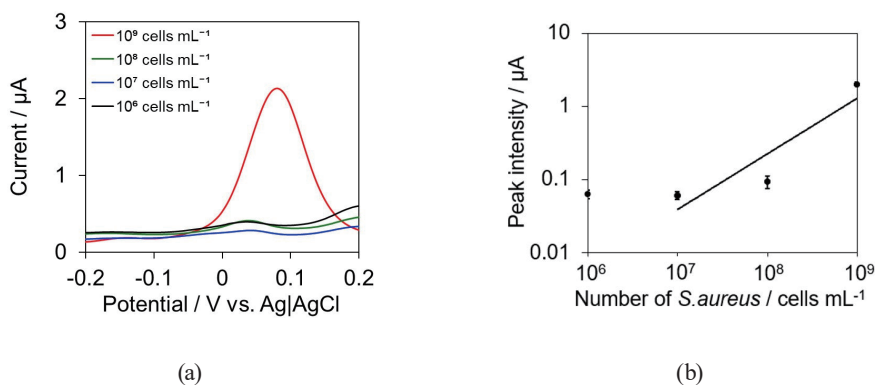


Fig. 5. (Color online) (a) DPV results of precipitate and (b) plot of peak current (I_p) at +0.08 V ($n = 3$).

operation, the absorption peak at 620 nm disappeared [Fig. 4(B-b)]. This change in absorbance was based on free and nonspecifically adsorbed labels obtained by removing labeled bacterial cells from the mixed dispersion [Fig. 4(B-a)]. Therefore, ΔI increased with the number of bacterial cells owing to the decrease in the number of labels not bound to the bacterial cells [$R^2 = 0.9997$, Fig. 4(B-c)]. In this way, we succeeded in the spectroscopic quantification of target bacteria by focusing on labels that did not specifically bind.

In the DPV of labeled bacterial cells obtained as precipitates, the current response resulting from the oxidation of copper nanostructures was obtained at +0.08 V [Fig. 5(a)]. The peak current (I_p), based on the number of labels bound to *S. aureus* on the electrode, increased with the number of bacterial cells [$R^2 = 0.9850$, Fig. 5(b)]. On the basis of this result, the electrochemical quantification of specifically bound labels was also successful.

4. Conclusions

We have developed copper nanostructures with characteristic spectroscopic and electrochemical properties and clarified that they function as labels by introducing antibodies into these structures. Complementary results were obtained by evaluating supernatants and precipitates from mixtures of labels and target bacterial cells. Therefore, it was clarified that the use of such labels enables the detection of target bacterial cells by spectroscopic and electrochemical techniques. However, the detection limits of both techniques were not satisfactory. In the future, it will be necessary to investigate the increase in the number of copper nanoparticles in the nanostructures. Since this method can respond to various target bacterial cells by introducing antibodies into nanostructures, it is useful for measuring various bacteria that cause not only food poisoning but also infectious diseases.

Acknowledgments

We gratefully acknowledge the financial support provided by a JST START Grant (Number JPMJST1916). We also acknowledge the financial support from the Japan Society for the

Promotion of Science Grant-in-Aid for Scientific Research (A) (KAKENHI 21H04963) and Grant-in-Aid for Challenging Exploratory Research (22K18442).

References

- 1 S. P. Oliver, B. M. Jayarao, and R. A. Almeida: Foodborne Pathog. Dis. **2** (2005) 115. <https://doi.org/10.1089/fpd.2005.2.115>
- 2 H. P. Dwivedi and L. A. Jaykus: Crit. Rev. Microbiol. **37** (2011) 40. <https://doi.org/10.3109/1040841X.2010.506430>
- 3 E. C. Alocilja and S. M. Radke: Biosens. Bioelectron. **18** (2003) 841. [https://doi.org/10.1016/S0956-5663\(03\)00009-5](https://doi.org/10.1016/S0956-5663(03)00009-5)
- 4 S. Chemburu, E. Wilkins, and I. Abdel-Hamid: Biosens. Bioelectron. **21** (2005) 491. <https://doi.org/10.1016/j.bios.2004.11.025>
- 5 X. Zhao, C. W. Lin, J. Wang, and D. H. Oh: J. Microbiol. Biotechnol. **24** (2014) 297. <https://doi.org/10.4014/jmb.1310.10013>
- 6 M. Du, J. Li, Q. Liu, Y. Wang, E. Chen, F. Kang, and C. Tu: Microbiol. Res. **251** (2021) 126838. <https://doi.org/10.1016/j.micres.2021.126838>
- 7 F. J. Loge, D. E. Thompson, and D. R. Call: Environ. Sci. Technol. **36** (2002) 2754. <https://doi.org/10.1021/es015777m>
- 8 T. R. DeCory, R. A. Durst, S. J. Zimmerman, L. A. Garringer, G. Paluca, H. H. DeCory, and R. A. Montagna: Appl. Environ. Microbiol. **71** (2005) 1856. <https://doi.org/10.1128/aem.71.4.1856-1864.2005>
- 9 S. Ikeda, K. Takabe, M. Inagaki, N. Funakoshi, and K. Suzuki: Pathol. Int. **57** (2007) 594. <https://doi.org/10.1111/j.1440-1827.2007.02144.x>
- 10 T. Planche, A. Aghaizu, R. Holliman, P. Riley, J. Poloniecki, A. Breathnach, and S. Krishna: Lancet Infect. **8** (2008) 777. [https://doi.org/10.1016/S1473-3099\(08\)70233-0](https://doi.org/10.1016/S1473-3099(08)70233-0)
- 11 S. L. Foley and K. Grant: Foodborne Diseases. (Springer, 2007) p. 485. https://doi.org/10.1007/978-1-59745-501-5_20
- 12 T. Wei, D. Du, M. J. Zhu, Y. Lin, and Z. Dai: Appl. Mater. Interfaces **8** (2016) 6329. <https://doi.org/10.1021/acsami.5b11834>
- 13 Y. Hu, Y. Sun, J. Gu, F. Yang, S. Wu, C. Zhang, X. Ji, H. Lv, S. Muyldermans, and S. Wang: Food Chem. **353** (2021) 129481. <https://doi.org/10.1016/j.foodchem.2021.129481>
- 14 C. Wang, Y. Xing, G. Zhang, M. Yuan, S. Xu, D. Liu, W. Chen, J. Peng, S. Hu, and W. H. La: Food Chem. **281** (2021) 91. <https://doi.org/10.1016/j.foodchem.2018.12.079>
- 15 L. Zhang, H. Huang, J. Wang, Y. Rong, W. Lai, J. Zhang, and T. Chen: Langmuir **31** (2015) 5537. <https://doi.org/10.1021/acs.langmuir.5b00592>
- 16 H. Shiigi, Y. Yamamoto, N. Yoshi, H. Nakao, and T. Nagaoka: Chem. Commun. **41** (2006) 4288. <https://doi.org/10.1039/B610085F>
- 17 H. Shiigi, R. Morita, Y. Yamamoto, S. Tokonami, H. Nakao, and T. Nagaoka: Chem. Commun. **24** (2009) 3615. <https://doi.org/10.1039/b903728d>
- 18 R. Morita, R. Inoue, S. Tokonami, Y. Yamamoto, M. Nakayama, H. Nakao, H. Shiigi, and T. Nagaoka: J. Electrochem. Soc. **158** (2011) K95. <https://doi.org/10.1149/1.3549166>
- 19 H. Shiigi, Y. Muranaka, Y. Hatsuoka, Y. Yamamoto, and T. Nagaoka: J. Electrochem. Soc. **160** (2013) H813. <https://doi.org/10.1149/2.058311jes>
- 20 H. Shiigi, M. Fukuda, T. Tono, K. Takada, T. Okada, D. Q. Le, Y. Hatsuoka, T. Kinoshita, M. Takai, S. Tokonami, H. Nakao, T. Nishino, Y. Yamamoto, and T. Nagaoka: Chem. Commun. **50** (2014) 6252. <https://doi.org/10.1039/c4cc01204f>
- 21 H. Shiigi, T. Kinoshita, M. Fukuda, D. Q. Le, T. Nishino, and T. Nagaoka: Anal. Chem. **87** (2015) 4042. <https://doi.org/10.1021/acs.analchem.5b00415>
- 22 S. Itagaki, S. Tanabe, H. Ikeda, X. Shan, S. Nishii, Y. Yamamoto, Y. Sadanaga, Z. Chen, and H. Shiigi: Analyst **147** (2022) 2355. <https://doi.org/10.1039/D2AN00475E>
- 23 S. Tanabe, S. Itagaki, K. Matsui, S. Nishii, Y. Yamamoto, Y. Sadanaga, and H. Shiigi: Anal. Chem. **94** (2022) 10984. <https://doi.org/10.1021/acs.analchem.2c01188>
- 24 L. Wen-Zhi and L. You-Qin: Sens. Actuators, B **141** (2009) 147. <https://doi.org/10.1016/j.snb.2009.05.037>